



HAL
open science

Heterogeneous ice nucleation activity of bacteria: new laboratory experiments at simulated cloud conditions

Ottmar Möhler, Dimitrios G. Georgakopoulos, Cindy E. Morris, S. Benz, V. Ebert, S. Hunsmann, H. Saathoff, M. Schnaiter, Richard Wagner

► **To cite this version:**

Ottmar Möhler, Dimitrios G. Georgakopoulos, Cindy E. Morris, S. Benz, V. Ebert, et al.. Heterogeneous ice nucleation activity of bacteria: new laboratory experiments at simulated cloud conditions. 2008. <hal-00330293>

HAL Id: hal-00330293

<https://hal.science/hal-00330293v1>

Preprint submitted on 18 Jun 2008

HAL is a multi-disciplinary open access archive for the deposit and dissemination of scientific research documents, whether they are published or not. The documents may come from teaching and research institutions in France or abroad, or from public or private research centers.

L'archive ouverte pluridisciplinaire **HAL**, est destinée au dépôt et à la diffusion de documents scientifiques de niveau recherche, publiés ou non, émanant des établissements d'enseignement et de recherche français ou étrangers, des laboratoires publics ou privés.



HAL Authorization

Biogeosciences Discussions is the access reviewed discussion forum of *Biogeosciences*

**Ice nucleation of
bacterial cells**

O. Möhler et al.

Heterogeneous ice nucleation activity of bacteria: new laboratory experiments at simulated cloud conditions

O. Möhler¹, D. G. Georgakopoulos², C. E. Morris³, S. Benz¹, V. Ebert⁴, S. Hunsmann⁴, H. Saathoff¹, M. Schnaiter¹, and R. Wagner¹

¹Institute for Meteorology and Climate Research (IMK-AAF), Forschungszentrum Karlsruhe, Karlsruhe, Germany

²Department of Agricultural Biotechnology, Agricultural University of Athens, Athen, Greece

³INRA, Unité de Pathologie Végétale UR407, Montfavet, France

⁴Institute for Physical Chemistry, University of Heidelberg, Heidelberg, Germany

Received: 11 February 2008 – Accepted: 10 March 2008 – Published: 7 April 2008

Correspondence to: O. Möhler (ottmar.moehler@imk.fzk.de)

Published by Copernicus Publications on behalf of the European Geosciences Union.

Title Page

Abstract

Introduction

Conclusions

References

Tables

Figures

◀

▶

◀

▶

Back

Close

Full Screen / Esc

Printer-friendly Version

Interactive Discussion



Abstract

The ice nucleation activities of five different *Pseudomonas syringae*, *Pseudomonas viridiflava* and *Erwinia herbicola* bacterial species and of Snomax™ were investigated in the temperature range between -5 and -15°C . Water suspensions of these bacteria were directly spray into the cloud chamber of the AIDA facility of Forschungszentrum Karlsruhe at a temperature of -5.7° . At this temperature, about 1% of the Snomax™ cells induced freezing of the spray droplets before they evaporated in the cloud chamber. The other suspensions of living cells didn't induce any measurable ice concentration during spray formation at -5.7° . The remaining aerosol was exposed to typical cloud activation conditions in subsequent experiments with expansion cooling to about -11°C . During these experiments, the bacterial cells first acted as cloud condensation nuclei to form cloud droplets and then eventually acted as ice nuclei to freeze the droplets. The results indicate that the bacteria investigated in the present study are mainly ice active in the temperature range between -7 and -11°C with an INA fraction of the order of 10^{-4} . The ice nucleation efficiency of Snomax™ cells was much larger with an INA fraction of 0.2 at temperatures around -8°C .

1 Introduction

Numerous organisms, including plants, invertebrates and microorganisms, can catalyze the freezing of supercooled water, i.e. they can act as heterogeneous ice nuclei. This property is generally due to the production of proteins or proteinaceous compounds (see Morris et al., 2004, for a review). Some of these proteins are particularly efficient ice nuclei, being able to induce freezing at temperatures just below 0°C , and are among the most active of the naturally occurring heterogeneous ice nuclei (Lee et al., 1995). Strains of the bacterium *Pseudomonas syringae*, in particular, can express ice nucleation activity at -1 or -2°C . The bacterium *Pseudomonas syringae* colonises plant surfaces from where it is emitted into the atmosphere. Net upward flux

BGD

5, 1445–1468, 2008

Ice nucleation of bacterial cells

O. Möhler et al.

Title Page

Abstract

Introduction

Conclusions

References

Tables

Figures

◀

▶

◀

▶

Back

Close

Full Screen / Esc

Printer-friendly Version

Interactive Discussion



**Ice nucleation of
bacterial cells**

O. Möhler et al.

[Title Page](#)[Abstract](#)[Introduction](#)[Conclusions](#)[References](#)[Tables](#)[Figures](#)[◀](#)[▶](#)[◀](#)[▶](#)[Back](#)[Close](#)[Full Screen / Esc](#)[Printer-friendly Version](#)[Interactive Discussion](#)

of *P. syringae* has been recorded at rates of about $30 \text{ m}^{-2} \text{ s}^{-1}$ above plant canopies (Lindemann et al., 1982). Such emission from plant canopies is apparently effective in transporting this bacterium up into clouds where it has been detected by several independent research teams (Sands et al., 1982; Amato et al., 2007). Ice nucleation active (INA) strains of *P. syringae* have also been detected in rain and snow (Constantinidou et al., 1990; Morris et al., 2008) and in diverse substrates outside of agricultural contexts suggesting that they are disseminated via the water cycle (Morris et al., 2008).

Because of the importance of the ice phase in clouds in the initiation of precipitation, a role for ice nucleation active bacteria in rain and snowfall has long been suspected (see Möhler et al., 2007, for a review). In fact it requires so-called ice nuclei, i.e. solid aerosol particles with specific surface properties, to freeze supercooled water droplets at temperatures above -35°C . Once formed, the ice phase in clouds growth and multiplies by a sequence of processes eventually leading to precipitation. As warmer the freezing temperature as more time the ice particles have to take part in this sequence and as more likely they grow to precipitation size. It was shown in previous studies that bacteria are candidates for effective ice nuclei at such warm temperatures (Maki et al., 1974; Vali et al., 1976; Yankofsky et al., 1981; Levin and Yankofsky, 1983; Ward and DeMott, 1989, see e.g.). Up to now it is however not clear which are the sources and concentrations of the species of most importance in cloud evolution and how efficient those species are in acting as ice nuclei under the conditions of atmospheric clouds. To address the latter question, new series of ice nucleation experiments with bacteria have been started in the AIDA (Aerosol Interaction and Dynamics in the Atmosphere) facility of Forschungszentrum Karlsruhe. Under humidity and temperature conditions of expanding cloud parcels, the ice nucleation efficiency of some selected *Pseudomonas syringae*, *Pseudomonas viridiflava* and *Erwinia herbicola* species were investigated at temperatures between -5 and -15°C . Experiments with Snomax™ have also been performed for comparison with previous studies (Ward and DeMott, 1989; Wood et al., 2002).

2 Preparation of bacterial cells

Two series of ice nucleation experiments, Bio02 and Bio03, were conducted with Snomax™ and 5 different strains of bacteria. All samples were prepared as suspensions in nanopure water for later dispersion of the bacterial cells into the aerosol phase (see Sect. 4). Table 1 summarises some properties of the six different suspensions. Snomax™ pellets from York Snow Inc. were used to prepare samples SM1 and SM2. Snomax™ is an industrial product of strain *P. syringae* 31R1 grown under conditions (industrial secret) to maximize the ice nucleation activity. Snomax™ is used to initiate snow formation behind water spray nozzles used by ski areas for ‘artificial’ snowmaking. The SM1 sample was prepared for the Bio02 experiments with a Snomax™ mass concentration of 1 mg ml^{-1} . After spraying 20 ml of SM1 into the 84 m^3 large aerosol vessel (see Sect. 4) the cell concentration was about 160 cm^{-3} (see Table 2). From this we can estimate a minimum cell concentration of $6.7 \times 10^8 \text{ ml}^{-1}$ in the SM1 sample. The SM2 sample prepared for Bio03 had a 10 times lower mass concentration than SM1. Dispersion of 50 ml resulted in a cell concentration of 40 cm^{-3} in the aerosol phase, from which we can calculate a minimum cell concentration of $6.7 \times 10^7 \text{ ml}^{-1}$ in the SM2 sample. We were not able to quantify the losses of cells during the dispersion, but a concentration of 1×10^9 bacterial cells in 1 mg of the Snomax™ pellets is a reasonable estimate.

For further ice nucleation experiments with living bacteria we selected strains that were known from previous studies to show high INA at warm temperature when grown appropriately. The samples have again be tested for their INA with the droplet freezing method as described in Sect. 3. Sample PS1 was prepared as a bacteria mixture of strain *Pseudomonas viridiflava* FMu 107 and *Pseudomonas syringae* IceHv. The first bacterium is a very close relative of *P. syringae* and is often difficult to distinguish from *P. syringae*. This strain was isolated from frosted Chinese cabbage at the onset of the period for frost risk (in storage and in the field) in Beijing, People’s Republic of China (Morris et al., 1992). The strain *P. syringae* IceHv was isolated from field-grown

BGD

5, 1445–1468, 2008

Ice nucleation of bacterial cells

O. Möhler et al.

Title Page

Abstract

Introduction

Conclusions

References

Tables

Figures

◀

▶

◀

▶

Back

Close

Full Screen / Esc

Printer-friendly Version

Interactive Discussion



barley in Avignon, France in the fall of 2005. Both samples were mixed together in order to get enough volume for several experiments with the same sample at different temperatures in the cloud simulation chamber (see Sect. 4). The strain *P. syringae* Cit7 was isolated from an orange tree in 1985, and *P. syringae* 31R1 from corn in 1976 by Lindow (1982). The latter is also used for the production of Snomax™. For preparing the bacteria suspensions, the cells were grown on petri dishes containing King's B agar (King et al., 1954) for 3 days at 25°C. Petri dishes were then transferred to 4°C and were stored for one week. We have observed that storage of the cells at this temperature for a few days enhances their ice nucleation activity. After this period of storage, they were washed off the plates with sterile distilled water, centrifuged to eliminate traces of the substrate and resuspended again in sterile distilled water. The suspension was adjusted to an optical density of 0.6 at a wavelength of 580 nm which corresponds to a cell number concentration of about $1 \times 10^9 \text{ ml}^{-1}$.

3 Droplet freezing experiments

The bacterial suspensions used for the Bio02 set of experiments were tested for their INA behaviour prior to the AIDA cloud simulation experiments. The INA was determined with the droplet freezing method, as described by Lindow (1982). Briefly, a set of 20 μl droplets from tenfold dilutions of a bacterial suspension is placed on a paraffin-coated aluminum foil, placed on a cooling bath. The temperature of the bath is then lowered and the number of frozen drops at each temperature (at 1° intervals after a 30 s delay) is recorded. By taking into account the concentration of bacteria, it is possible to estimate the concentration of ice nuclei for each temperature and, therefore, the ice nucleation-active proportion of the bacterial population. In this way we obtained for sample PS1 an INA cell number concentration of about $7 \times 10^3 \text{ ml}^{-1}$ at a temperature of -9°C . By dividing through the total cell concentration of $1 \times 10^9 \text{ ml}^{-1}$ we obtain from an INA cell fraction of 7×10^{-6} at the same temperature.

Title Page

Abstract

Introduction

Conclusions

References

Tables

Figures

◀

▶

◀

▶

Back

Close

Full Screen / Esc

Printer-friendly Version

Interactive Discussion



4 Cloud simulation experiments

The immersion and condensaton freezing efficiency of bacterial cells suspended in the aerosol phase was investigated at temperatures between -5 and -20°C . The experiments were performed in the AIDA (Aerosol Interaction and Dynamics in the Atmosphere) facility of Forschungszentrum Karlsruhe. ADIA can be operated as a pumped expansion chamber to investigate aerosol-cloud processes at simulated temperature and humidity conditions of atmospheric clouds (Möhler et al., 2005, 2006). Two series of experiments were performed during the AIDA campaigns Bio02 in January 2006 and Bio03 in May 2006 (see Table 2).

Briefly, the AIDA facility consists of a cylindrical aluminium vessel with a volume of 84 m^3 . As described later, this vessel was used as a cloud simulation chamber for the experimens discussed here. The vessel is located in a thermally insulating box. An air ventilation, heating, and cooling system controls the temperature inside this box in the range from 60 to -90°C . In preparation of the experiments, temperature changes are normally actuated during the night hours in order to approach the desired starting temperature at a rate of about 4 K/h . During the experiments, the cooling system is operated at constant and homogeneous temperature control with temporal and spatial variability below $\pm 0.3\text{ K}$ throughout the cold box and the cloud chamber. Also during the evening and night hours, the cloud chamber is cleaned by pumping to a pressure below 1 hPa , flushing with dry synthetic air, and filling with particle free humid air. The particle background after filling to atmospheric pressure is normally below 0.1 cm^{-3} . Experiments were started at a pressure between 1002 and 1021 hPa (see Table 2). At constant temperature and pressure conditions, a high relative humidity between 90 and 95% is maintained inside the cloud simulation chamber by a partial dew or, at lower wall temperatures, ice coverage of the inner chamber walls. The AIDA facility is equipped with a comprehensive set of water, aeerosol, and cloud instruments (Möhler et al., 2005, 2006). For the present study we used the chilled mirror frost point hygrometer LX-373 from MBW Calibration Ltd. in Switzerland for total water concentration

BGD

5, 1445–1468, 2008

Ice nucleation of bacterial cells

O. Möhler et al.

Title Page

Abstract

Introduction

Conclusions

References

Tables

Figures

◀

▶

◀

▶

Back

Close

Full Screen / Esc

Printer-friendly Version

Interactive Discussion



measurements, the tunable diode laser absorption spectrometer APicT-DLAS (Ebert et al., 2005) for fast and sampling-free open-path water vapour measurements inside the AIDA vessel, the in situ light scattering and depolarisation setup SIMONE for the sensitive detection of droplet and ice particle growth, the infrared extinction spectrometer (FTIR) for the characterisation of droplet and ice particles (Wagner et al., 2006), two optical particle counters Welas from Palas GmbH in Karlsruhe, Germany for measuring the number concentrations of droplets and ice particles (Benz et al., 2005), as well as two condensation particle counters (CPC3010, CPC3025), the scanning mobility particle sizer (SMPS) and the aerodynamic particle spectrometer (APS) from TSI Inc. for aerosol measurements.

Figure 1 schematically shows the experimental setup for aerosol formation and characterisation. Bacterial suspensions were prepared as described in Sect. 2 and directly sprayed into the cloud chamber. It took a few minutes to disperse the sample volume V_s which ranged from 20 to 100 ml (see Table 2). Thus, the bacterial cells were first immersed in water droplets when entering the cloud chamber. The dispersion nozzle was heated to about 20°C, but the droplets quickly cooled to the temperature of the cloud chamber volume and then started to evaporate. Eventually, the bacterial cells acted as ice nuclei in the immersion mode before the droplet completely evaporated. This immersion freezing effect during spray formation of the bacterial aerosol will be discussed in Sect. 5.

After all the droplets evaporated within about 5 to 10 min, the resulting aerosol size distributions were measured with the SMPS and APS aerosol instruments. Both instruments were operated outside the cold box (Fig. 1) and connected to the cloud chamber with stainless steel sampling tubes. Particle losses in the sampling tubes can be neglected for the particle size range of interest in the present study. It should be noted here that the SMPS system measures the electrical mobility size and the APS the aerodynamic size of aerosol particles. Both diameters are different for particles which are nonspherical, and therefore have a dynamic shape factor larger than one, or which have a density different from 1 g cm^{-3} . Because bacterial cells are known

Ice nucleation of bacterial cells

O. Möhler et al.

[Title Page](#)[Abstract](#)[Introduction](#)[Conclusions](#)[References](#)[Tables](#)[Figures](#)[◀](#)[▶](#)[◀](#)[▶](#)[Back](#)[Close](#)[Full Screen / Esc](#)[Printer-friendly Version](#)[Interactive Discussion](#)

**Ice nucleation of
bacterial cells**O. Möhler et al.

[Title Page](#)[Abstract](#)[Introduction](#)[Conclusions](#)[References](#)[Tables](#)[Figures](#)[◀](#)[▶](#)[◀](#)[▶](#)[Back](#)[Close](#)[Full Screen / Esc](#)[Printer-friendly Version](#)[Interactive Discussion](#)

to be nonspherical, the SMPS and APS diameters were converted into the so-called volume-equivalent sphere diameter, i.e. the diameter of a spherical particle having the same terminal settling velocity as the particles measured with the SMPS and APS. Best match of the transferred SMPS and APS size distributions was achieved with a density of 1 g cm^{-3} and a dynamic shape factor of about 1.1 to 1.3. The nonspherical nature of the bacterial cells in the aerosol phase was also reflected by an enhanced depolarisation ratio of scattered light measured with SIMONE during and after adding the bacterial cells to the cloud chamber (see Sect. 5). Figures 2 and 3 show two examples of size distributions measured before the start of experiments Bio03_07 and Bio03_09, respectively. Both examples reveal the clear bimodal structure of the aerosol which was observed in all experiments. The reason for that is the fact that only a minor fraction of the droplets generated by the spray nozzle contained a bacterial cell. The mode of smaller particles can therefore be explained as residual particles of evaporating droplets without a bacterial cell. The smaller but more narrow mode of larger particles shows the size distribution of the bacterial cells in the aerosol phase. The larger mode size of about $0.8 \mu\text{m}$ for Snomax™ (Fig. 2) and $0.6 \mu\text{m}$ for *P. syringae* 31R1 (Fig. 3) is in good agreement with the expected size of single bacterial cells.

In some cases the larger mode of cell particles showed a tail towards larger particle diameters. This can be explained by a minor fraction of agglomerate particles of 2 or more bacterial cells originating from larger droplets which contained the respective number of cells after dispersion. The formation of larger cell agglomerates by coagulation in the aerosol phase in the cloud chamber can be neglected for the number concentrations of cell particles (see below) on the time scales of the experiments. A bimodal lognormal size distribution was fitted to the measured data, shown as solid lines in Figs. 2 and 3. The number concentration n_{ae} of the total aerosol, i.e. the sum of both modes, and the number concentration n_{cells} of the bacterial cells in the larger mode were obtained from the lognormal fits. The results are listed in Table 2. The size distribution fit result for n_{ae} was in good agreement with the aerosol number concentrations directly measured with the condensation particle counter CPC3025 and, for

number concentrations below about $10\,000\text{ cm}^{-3}$ also with the CPC3010 instrument. With number concentration between about 30 and 300 cm^{-3} the bacterial cells in the cloud chamber were about a factor 6 to 60 less abundant than the residual particles.

The efficiency of the bacterial cells in the condensation and immersion modes of freezing was investigated in dynamic expansion experiments. Time series of pressure, temperature, relative humidity, as well as aerosol, droplet, and ice particle number concentrations are depicted in Figs. 4 and 5 for the expansion experiments Bio03_07 and Bio03_09, respectively. The expansion experiments were started after aerosol generation at constant pressure and temperature conditions as given in Table 2. The pressure in the cloud chamber was then lowered by pumping to about 850 hPa within a time period of about 5 min (solid black line in top panel). The time axis in Figs. 4 and 5 is plotted in seconds relative to start pumping. In all expansion experiments the same expansion rate was achieved by setting the pump speed to 60% of its maximum value. The pump speed is also indicated in Table 2. A value of 0 indicates the spray dispersion experiments at constant pressure and temperature and a value of 60 the expansion experiments with dynamic changes of pressure, temperature, and humidity. The pumping expansion causes adiabatic cooling of the cloud chamber volume shown by the measured gas temperature T_g in Figs. 4 and 5 (solid blue line in top panel). A mixing fan in the bottom part of the chamber volume forces homogeneous temperature and humidity conditions during the expansion. The wall temperature T_w (dash-dotted line in top panel) stays almost constant all the time. The increasing difference between T_w and T_g causes an increasing heat flux from the chamber walls and thereby an increasing deviation of the temperature profile from the adiabatic case.

The relative humidities RH with respect to water (solid blue line in second panel of Figs. 4 and 5) are obtained from water vapour concentrations measured by in situ high-resolution diode laser absorption spectroscopy (APicT-DLAS) and the saturation vapour pressures of water calculated for T_g . The water vapor concentrations were measured directly within the cloud by using a fibre-coupled, open-path, White-type absorption cell with an absorption path length of 23.6 m inside the cloud chamber (see

Ice nucleation of bacterial cells

O. Möhler et al.

Title Page

Abstract

Introduction

Conclusions

References

Tables

Figures

◀

▶

◀

▶

Back

Close

Full Screen / Esc

Printer-friendly Version

Interactive Discussion



Mangold et al., 2005, for more details). During the Bio02 and Bio03 experiments the APicT-DLAS measured with a 1.5 s temporal resolution and a concentration resolution of about 20 ppm. Starting from about 95%, the relative humidity increases due to the expansion cooling and approaches water saturation after about 40 s of pumping. At about the same time, the total number of particles measured with the optical particle counter Welas (grey line in the lower panel) steeply raises due to the activation and growth of water droplets. The FTIR extinction spectra measured at the same time (not shown in the figure) reveal that initially only water droplets are formed and that the number of droplets is close to the number of aerosol particles before droplet formation (black line in the lower panel). It should be noted that the CPC3010 measures the total particle concentration and does not distinguish between aerosol particles and droplets. The Welas instrument underestimates the total droplet concentration because some droplets are too small for optical detection. After 50 s of pumping, the mean droplet diameter was about 2 μm for experiment Bio03_07 and 3 μm for experiment Bio03_09.

The third panel of Figs. 4 and 5 show the SIMONE depolarisation ratio (SDR) of polarised laser light of 488 nm wavelength scattered from particles in the center of the cloud chamber to a scattering angle of 176°. Any SDR signal larger than the background level of about 0.04 clearly indicates the presence of nonspherical particles in the cloud chamber. These can be either bacterial cells, which are known to be aspherical, or ice particles growing to larger sizes after their nucleation by INA bacteria immersed in droplets. The SDR signals before start pumping, i.e. before cloud droplet and ice activation, are due to the bacterial cells alone. It can be seen in Figs. 4 and 5 that the *P. Syringae* bacteria of strain 31R1 gives a larger SDR than the Snomax™ cells, which means that the living cells are more aspherical. The number of ice particles formed during the expansion experiments was measured with the two optical particle counters Welas and Welas2 (blue circles and triangles, respectively, in the lower panel of Figs. 4 and 5). Both instruments are located below the cloud chamber and measure the concentration of ice particles larger than about 0.5 μm in a sample flow taken from the chamber volume through a vertical stainless steel sampling tube. In Table 2

BGD

5, 1445–1468, 2008

Ice nucleation of bacterial cells

O. Möhler et al.

Title Page

Abstract

Introduction

Conclusions

References

Tables

Figures

◀

▶

◀

▶

Back

Close

Full Screen / Esc

Printer-friendly Version

Interactive Discussion



are listed the maximum ice number concentrations measured during the respective experiments. The detection limit of the Welas instruments is about 0.1 cm^{-3} .

5 Results and discussion

Experimental parameters and results are summarised in Table 2. Most of the experiments were started at an initial temperature T_g of about -5.7°C . Only experiments Bio02_09 and Bio02_10 were started at a colder temperature of about -9.7°C . The amount of sample volume V_s sprayed into the cloud chamber is also given in Table 2 for the static experiments without pumping (zero pump speed). A zero volume indicates that the aerosol generated during the spray experiment before remained in the chamber for the subsequent expansion experiment. It was discussed in Sect. 4 how the number concentrations of total aerosol particles n_{ae} , bacterial cells n_{cells} , and ice particles n_i were measured. As a main result from this work, the ice nucleation active (INA) cell fraction f_{INA} was calculated from the ratio of n_i to n_{cells} . In case of the spray experiments with Snomax™ at -5.7°C , significant ice formation was only measured during Bio02_04 with an INA fraction of about 1%. For Bio03_06 only an upper limit of 0.003 could be given. This means that only 1% or less of the Snomax™ cells is ice-active at -5.7°C in the immersion mode of freezing, at least within the evaporation timescale of the spray droplets which is of the order of a few seconds to a few minutes. In similar cloud expansion studies with Snomax™ Ward and DeMott (1989) found some INA cells at a temperature around -5°C .

Figure 4 shows, as an illustration example, how the number of ice particles increased during the expansion experiment Bio03.07 after droplets had formed. The formation of some ice crystals immediately after the activation of the first droplets is indicated in a small SDR peak next to the vertical blue line. The number of ice crystals was below the detection limit of the Welas instruments. The SDR then drops and approaches the background value because the few ice crystals rapidly grew to large sizes and settled to the floor of the cloud chamber. The major peak of ice formation occurred between

Title Page

Abstract

Introduction

Conclusions

References

Tables

Figures

◀

▶

◀

▶

Back

Close

Full Screen / Esc

Printer-friendly Version

Interactive Discussion



**Ice nucleation of
bacterial cells**

O. Möhler et al.

Title Page

Abstract

Introduction

Conclusions

References

Tables

Figures

◀

▶

◀

▶

Back

Close

Full Screen / Esc

Printer-friendly Version

Interactive Discussion



50 and 110 s of pumping time with the Welas ice number concentration increasing to a maximum value of 10 cm^{-3} . This corresponds to an increase of fraction of INA cells from almost 0 to a maximum value of 0.23 within a narrow temperature range from about -7 to -9°C . At the same time, the depolarisation ratio starts to rise again, which also indicates the formation and growth of further ice crystals. About 20 s after the ice particle concentration reached its maximum value, the droplets evaporated due to the so-called Bergeron-Findeisen mechanism. In other words, the lower saturation pressure of water above the ice particles compared to the supercooled water droplets lowers the relative humidity, as also indicated in the TDL measurements, and therefore induces growth of the ice volume in expense of the liquid droplet. The evaporation of the droplets is also indicated in the steep SDR increase. After all water droplets evaporated, which was approved by the FTIR measurements, the pumping expansion still continued to a minimum temperature of about -11°C , but no further increase of n_i was observed. This indicates that the remaining 80% of the not yet INA cells didn't show strong INA in the deposition mode of ice nucleation at temperatures as low as -11°C . The ice number concentration increased with time due to settling losses of the larger ice crystals in the chamber, and about 150 s after pumping stopped the remaining ice crystals completely evaporated in the warming cloud chamber. Experiment Bio03_04 also revealed that about 20% of the Snomax™ cells are ice active between -7 and -9°C . This is in agreement to studies by Ward and DeMott (1989) and Wood et al. (2002) who also found strong ice nucleation efficiency of Snomax™ at these temperatures.

During experiment Bio03.09, ice particles also formed between about 50 and 110 s of pumping time (lowest panel in Fig. 5), but with a tenfold lower number concentration. In this experiment, the initially higher SDR of the more aspherical bacteria (see above) dropped to almost the background value during the formation of the liquid cloud. This indicates that at least most of the bacterial cells are CCN active and transform from aspherical particles to spherical droplets without scattering depolarisation. The SDR rises again along with the formation of ice particles and decreases with the depositional loss of the ice particles between 150 and 400 s. It should be noted that for the analysis

**Ice nucleation of
bacterial cells**

O. Möhler et al.

Title Page

Abstract

Introduction

Conclusions

References

Tables

Figures

◀

▶

◀

▶

Back

Close

Full Screen / Esc

Printer-friendly Version

Interactive Discussion



of f_{INA} in the present study we assumed that only the cell particles but not the residual particles are ice-active and, in case of the expansion experiments, that most of the cell particles were activated to form cloud droplets. The first assumption was supported by the fact that no significant ice formation was observed at temperature between -5.7 and -11°C in an expansion experiment with a filtered SnomaxTM suspension. The second assumption also seems to be reasonable because bacterial cells have found to be active cloud condensation nuclei at relatively low supersaturation with respect to water (Franc and DeMott, 1998; Bauer et al., 2003). So, at least if the cells are wettable, they are in favour for CCN activation due to their larger size compared to the residual particles. As discussed above also the SDR data indicates the CCN activation of bacterial cells.

In all spray experiments with living cells at -5.7°C no significant ice formation was observed. During the expansion experiments the same strains were only slightly active at temperatures between -7 and -11°C with INA fractions of the order of 10^{-4} . The lower ice-active fraction is also illustrated for experiment Bio03_09 in Fig. 5 which shows the same timeseries as already discussed above for experiment Bio03_07. For the PS1 sample a second spray experiment was performed at a temperature of -9.7°C . At this temperature the observed INA fraction was about 0.005 which is in good agreement to the value of 0.004 measured during the expansion experiment before at a similar temperature. This shows that the spray and expansion experiments are consistent and can be compared to each other. Surprisingly, no significant ice formation was observed in the expansion experiment Bio02_10 with cooling to a minimum temperature of -15.2°C . This indicates that almost all INA cells have been activated during the experiment Bio02_09 before, followed by either deactivation if the INA sites or removal from the cloud chamber by settling ice crystals. It was not possible to exactly determine the removal efficiency of ice crystals under the conditions of the experiments discussed here. At least a minor fraction of the ice particles formed during the expansion experiments with SnomaxTM were likely to evaporate in the chamber (see Fig. 4) and to release their ice nuclei to the chamber aerosol. Again, subsequent expansion

with the remaining aerosol not listed in Table 2 didn't show any significant ice formation. Further experiments are needed to investigate and quantify a possible deactivation effect of INA cells. We can conclude from experiments Bio02.06 to Bio02.10 that the ice nucleation activity of strains *P. viridiflava* FMu107 and *P. syringae* IceHv only occurs in a narrow temperature range around -10°C . Previous studies by Levin and Yankofsky (1983) and Ward and DeMott (1989) have also demonstrated that freezing induced by bacterial cells may occur only in narrow temperature ranges. For the sample PS1, the fraction of INA cells was also determined with the droplet freezing method as described in Sect. 3. The lower value of about 10^{-5} (the ratio between the number of INA cells and the number of cells per ml in Table 1) compared to the AIDA could be due to the slightly warmer temperature. However, further droplet freezing and AIDA chamber experiments are needed for a better quantitative comparison of both methods. This is in particular important because previous laboratory experiments on the ice nucleation efficiency of bacterial cells have also indicated INA fraction of the order of 10^{-5} (Yankofsky et al., 1981).

6 Conclusions

The ice nucleation efficiencies of five different *P. syringae*, *P. viridiflava* and *E. herbicola* bacteria strains were investigated at simulated cloud conditions in the temperature range from -5.7 to -15°C . No significant ice activity of the bacteria species was observed above -7°C . The results indicate that the bacteria investigated in the present study are mainly ice-active in the temperature range between -7 and -11°C with an INA fraction of the order of 10^{-4} . For the *P. syringae* strain 31R1, we measured an INA fraction of 4×10^{-4} at -10°C in AIDA experiments, but only 4×10^{-6} at -9°C in a freezing experiment with droplets deposited on an aluminium foil. From the experiments of the present study we are not able to conclude if this difference is only due to the slightly different temperature. Further comparison experiments are needed to investigate if there is a systematic difference between AIDA results and the droplet

Title Page

Abstract

Introduction

Conclusions

References

Tables

Figures

◀

▶

◀

▶

Back

Close

Full Screen / Esc

Printer-friendly Version

Interactive Discussion



freezing method according to [Lindow \(1982\)](#). For Snomax™ cells an INA fraction of about 0.2 was measured at temperatures around -8°C . A little ice activity was also observed around -6°C . The AIDA results are in reasonable agreement with [Ward and DeMott \(1989\)](#) who reported two distinct peaks of Snomax™ ice activity around -5 and -8°C . Some of the AIDA results indicate a possible deactivation of bacterial cells as active ice nuclei during the first ice activation event. Such a deactivation could have a remarkable impact on the role of INA bacteria in cloud formation and should further be investigated.

Acknowledgements. The authors are appreciative to the AIDA operators and technicians for their skilful support during the Bio02 and Bio03 campaigns. We also acknowledge support from T. Schwartz for preparing the biological samples in the microbiology lab of the Institute for Technical Chemistry of Forschungszentrum Karlsruhe, and from S. Wagner for assisting the programming and data analysis of the APicT-DLAS system. This work was funded within the Helmholtz Research Programme Atmosphere and Climate and contributes to the Helmholtz Virtual Institute on Aerosol-Cloud Interactions (VI-ACI).

References

- Amato, P., Parazols, M., Sancelme, M., Laj, P., Mailhot, G., and Delort, A. M.: Microorganisms isolated from the water phase of tropospheric clouds at the Puy de Dome: major groups and growth abilities at low temperatures, *FEMS Microbiology Ecology*, 59, 242–254, 2007. [1447](#)
- Bauer, H., Giebl, H., Hitzenberger, R., Kasper-Giebl, A., Reischl, G., Zibuschka, F., and Puxbaum, H.: Airborne bacteria as cloud condensation nuclei, *J. Geophys. Res.-Atmos.*, 108, 4658, doi:10.1029/2003JD003545, 2003. [1457](#)
- Benz, S., Megahed, K., Möhler, O., Saathoff, H., Wagner, R., and Schurath, U.: T-dependent rate measurements of homogeneous ice nucleation in cloud droplets using a large atmospheric simulation chamber, *J. Photoch. Photobio. A*, 176, 208–217, 2005. [1451](#)
- Constantinidou, H. A., Hirano, S. S., Baker, L. S., and Upper, C. D.: Atmospheric Dispersal of Ice Nucleation-Active Bacteria – the Role of Rain, *Phytopathology*, 80, 934–937, 1990. [1447](#)
- Ebert, V., Teichert, H., Giesemann, C., Saathoff, H., and Schurath, U.: Fiber-coupled in-situ

BGD

5, 1445–1468, 2008

Ice nucleation of bacterial cells

O. Möhler et al.

Title Page

Abstract

Introduction

Conclusions

References

Tables

Figures

◀

▶

◀

▶

Back

Close

Full Screen / Esc

Printer-friendly Version

Interactive Discussion



- laser absorption spectrometer for the selective detection of water vapour traces down to the ppb-level, *Technisches Messen*, 72, 23–30, 2005. [1451](#)
- Franc, G. D. and DeMott, P. J.: Cloud activation characteristics of airborne *Erwinia carotovora* cells, *J. Appl. Meteorol.*, 37, 1293–1300, 1998. [1457](#)
- 5 King, E. O., Ward, M. N., and Raney, D. T.: Two simple media for the demonstration of pyocyanin and fluorescein, *J. Lab. Clin. Med.*, 44, 301–307, 1954. [1449](#)
- Lee, R. E., Warren, G. J., and Gusta, L. V.: *Biological Ice Nucleation and Its Applications*, APS Press; The American Phytopathological Society, St. Paul, Minnesota, 1995. [1446](#)
- 10 Levin, Z. and Yankofsky, S. A.: Contact Versus Immersion Freezing of Freely Suspended Droplets by Bacterial Ice Nuclei, *J. Appl. Meteorol.*, 22, 1964–1966, 1983. [1447](#), [1458](#)
- Lindemann, J., Constantinidou, H. A., Barchet, W. R., and Upper, C. D.: Plants as a source of airborne bacteria, including ice nucleation active bacteria, *Appl. Environ. Microbiol.*, 44, 1059–1063, 1982. [1447](#)
- Lindow, S. E.: Population dynamics of epiphytic ice nucleation active bacteria on frost sensitive plants and frost control by means of antagonistic bacteria, in: *Plant Cold Hardiness and Freezing Stress*, edited by: Sakai, A. and Li, P. H., 2, Academic Press, New York, 1982. [1449](#), [1459](#)
- 15 Maki, L. R., Galyan, E. L., Chang-Chien, M. M., and Caldwell, D. R.: Ice nucleation induced by *Pseudomonas syringae*, *Appl. Environ. Microb.*, 28, 456–459, 1974. [1447](#)
- 20 Mangold, A., Wagner, R., Saathoff, H., Schurath, U., Giesemann, C., Ebert, V., Kramer, M., and Möhler, O.: Experimental investigation of ice nucleation by different types of aerosols in the aerosol chamber AIDA: implications to microphysics of cirrus clouds, *Meteorol. Z.*, 14, 485–497, 2005. [1454](#)
- Möhler, O., Büttner, S., Linke, C., Schnaiter, M., Saathoff, H., Stetzer, O., Wagner, R., Krämer, M., Mangold, A., Ebert, V., and Schurath, U.: Effect of sulfuric acid coating on heterogeneous ice nucleation by soot aerosol particles, *J. Geophys. Res.-Atmos*, 110, D11210, doi:10.1029/2004JD005169, 2005. [1450](#)
- 25 Möhler, O., Field, P. R., Connolly, P., Benz, S., Saathoff, H., Schnaiter, M., Wagner, R., Cotton, R., Krämer, M., Mangold, A., and Heymsfield, A. J.: Efficiency of the deposition mode ice nucleation on mineral dust particles, *Atmos. Chem. Phys.*, 6, 3007–3021, 2006, <http://www.atmos-chem-phys.net/6/3007/2006/>. [1450](#)
- 30 Möhler, O., DeMott, P. J., Vali, G., and Levin, Z.: Microbiology and atmospheric processes: the role of biological particles in cloud physics, *Biogeosciences*, 4, 1059–1071, 2007,

BGD

5, 1445–1468, 2008

Ice nucleation of bacterial cellsO. Möhler et al.

Title Page

Abstract

Introduction

Conclusions

References

Tables

Figures

◀

▶

◀

▶

Back

Close

Full Screen / Esc

Printer-friendly Version

Interactive Discussion



<http://www.biogeosciences.net/4/1059/2007/>. 1447

Morris, C. E., Wen, A.-M., Xu, X.-H., and Di, Y.-B.: Ice nucleation active bacteria on Chinese cabbage in northern China : populations dynamics and characteristics and their possible role in storage decay, *Phytopathology*, 82, 739–746, 1992. 1448

5 Morris, C. E., Georgakopoulos, D. G., and Sands, D. C.: Ice nucleation active bacteria and their potential role in precipitation, *J. Phys. IV*, 121, 87–103, 2004. 1446

Morris, C. E., Sands, D. C., Vinatzer, B. A., Glaux, C., Guilhaud, C., Buffière, A., Yan, S., Dominguez, H., and Thompson, B. M.: The life history of the plant pathogen *Pseudomonas syringae* is linked to the water cycle, *ISME Journal*, 2, 321–334, doi:10.1038/ismej.2007.113, 2008. 1447

10 Sands, D. C., Langhans, V. E., Scharen, A. L., and Smet, G.: The association between bacteria and rain and possible resultant meteorological implications, *J. Hungarian Meteorol. Serv.*, 86, 148–152, 1982. 1447

15 Vali, G., Christensen, M., Fresh, R. W., Galyan, L. R., Maki, L. R., and Schnell, R. C.: Biogenic Ice Nuclei. Part II: Bacterial Sources, *J. Atmos. Sci.*, 33, 1565–1570 , doi:10.1175/1520-0469(1976)033, 1976. 1447

Wagner, R., Benz, S., Möhler, O., Saathoff, H., and Schurath, U.: Probing ice clouds by broadband mid-infrared extinction spectroscopy: case studies from ice nucleation experiments in the AIDA aerosol and cloud chamber, *Atmos. Chem. Phys.*, 6, 4775–4800, 2006, <http://www.atmos-chem-phys.net/6/4775/2006/>. 1451

20 Ward, P. J. and DeMott, P. J.: Preliminary experimental evaluation of Snomax, *Pseudomonas syringae*, as an artificial ice nucleus for weather modification, *J. Wea. Mod.*, 21, 9–13, 1989. 1447, 1455, 1456, 1458, 1459

25 Wood, S. E., Baker, M. B., and Swanson, B. D.: Instrument for studies of homogeneous and heterogeneous ice nucleation in free-falling supercooled water droplets, *Rev. Sci. Instrum.*, 73, 3988–3996, 2002. 1447, 1456

Yankofsky, S. A., Levin, Z., Bertold, T., and Sandlerman, N.: Some basic characteristics of bacterial freezing nuclei, *J. Appl. Meteorol.*, 20, 1013–1019, 1981. 1447, 1458

BGD

5, 1445–1468, 2008

Ice nucleation of bacterial cells

O. Möhler et al.

Title Page

Abstract

Introduction

Conclusions

References

Tables

Figures

◀

▶

◀

▶

Back

Close

Full Screen / Esc

Printer-friendly Version

Interactive Discussion



Ice nucleation of bacterial cells

O. Möhler et al.

Table 1. Overview of samples prepared for the experiments. The cell number concentration was obtained from microscopic analysis for the Snomax™ suspensions and from optical density measurements for the living cell suspensions.

Sample	Type of bacteria	Cell concentration (ml^{-1})
SM1	Snomax™	1×10^9
SM2	Snomax™	1×10^8
PS1	<i>P. viridiflava</i> FMu107 <i>P. syringae</i> IceHv	1×10^9
PS2	<i>P. syringae</i> 31R1	1×10^9
PS3	<i>P. syringae</i> Cit7	1×10^9
EH1	<i>E. herbicola</i> 268 Rb-2	9×10^8

Title Page

Abstract

Introduction

Conclusions

References

Tables

Figures

◀

▶

◀

▶

Back

Close

Full Screen / Esc

Printer-friendly Version

Interactive Discussion



Table 2. Parameters of AIDA experiments and measured ice active fractions of bacterial cells. V_s is the sample volume of the bacterial suspension directly sprayed into the AIDA cloud chamber at the beginning of the respective experiments. The resulting aerosol remained in the chamber for the following experiment with expansion cooling by pumping. p and T_g are the initial pressure and temperature in the cloud chamber, and n_{ae} , n_{cells} , and n_i the measured number concentrations of total aerosol, bacterial cell, and ice particles, respectively. The ice active cell fraction f_{INA} is the ratio of n_i to n_{cells} , and T_i the temperature at which the peak of ice formation was observed.

Type of experiment				Initial parameters				Ice nucleation results		
Exp. key	Bacteria sample	V_s ml	Pump speed (%)	p hPa	T_g °C	n_{ae} cm ⁻³	n_{cells} cm ⁻³	n_i cm ⁻³	f_{INA}	T_i °C
Bio02.04	SM1	20	0	1020.8	-5.6	5500	160	2	0.01	-5.6
Bio02.05	SM1	0	60	1020.0	-5.7	4450	150	40	0.2	-8±1
Bio02.06	PS1	20	0	1010.0	-5.8	18 000	290	<0.1	<0.0003	-5.8
Bio02.07	PS1	0	60	1008.0	-5.9	17 000	275	1	0.004	-10±1
Bio02.09	PS1	20	0	1002.1	-9.7	12 800	300	1	0.005	-9.7
Bio02.10	PS1	0	60	1002.0	-9.8	12 250	280	<0.1	<0.0004	-13±3
Bio03.06	SM2	50	0	1005.0	-5.7	13 300	38	<0.1	<0.003	-5.7
Bio03.07	SM2	0	60	1005.1	-5.8	11 700	43	10	0.23	-8±1
Bio03.08	PS2	50	0	1006.0	-5.6	4800	311	<0.1	<0.0003	-5.6
Bio03.09	PS2	0	60	1005.9	-5.7	4400	316	1	0.0032	-8±1
Bio03.11	PS3	50	0	1005.0	-5.7	6300	195	<0.1	<0.0005	-5.7
Bio03.12	PS3	0	60	1005.1	-5.8	4900	155	0.2	0.0013	-8±1
Bio03.19	EH1	100	0	1008.0	-5.7	2736	177	<0.1	<0.0006	-5.7
Bio03.20	EH1	0	60	1008.0	-5.8	2455	150	0.1	0.0007	-9±1

Ice nucleation of bacterial cells

O. Möhler et al.

Title Page

Abstract

Introduction

Conclusions

References

Tables

Figures

◀

▶

◀

▶

Back

Close

Full Screen / Esc

Printer-friendly Version

Interactive Discussion



Ice nucleation of bacterial cells

O. Möhler et al.

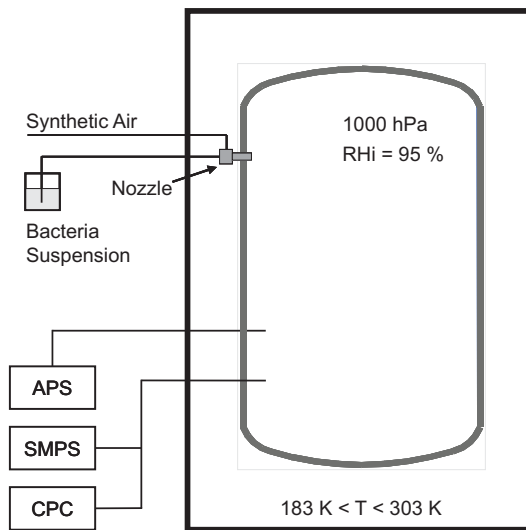


Fig. 1. Schematic of experimental setup for aerosol generation and characterisation.

Title Page

Abstract

Introduction

Conclusions

References

Tables

Figures

◀

▶

◀

▶

Back

Close

Full Screen / Esc

Printer-friendly Version

Interactive Discussion



Ice nucleation of
bacterial cells

O. Möhler et al.

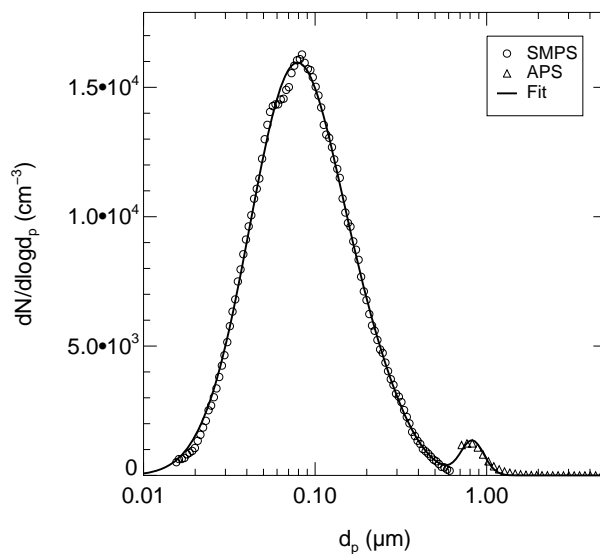


Fig. 2. Size distribution of Snomax™ aerosol measured before expansion experiment Bio03_07 with the scanning mobility particle spectrometer SMPS (circles) and the aerodynamic particle spectrometer APS (triangles). The size distribution clearly reveals the bi-modal nature of the aerosol with smaller residual particles from evaporated droplets which didn't contain intact bacterial cells, and the larger, but less abundant, bacterial cell particles with diameters around $0.8 \mu\text{m}$. A bimodal lognormal size distribution (solid line) was fitted to the data.

[Title Page](#)[Abstract](#)[Introduction](#)[Conclusions](#)[References](#)[Tables](#)[Figures](#)[◀](#)[▶](#)[◀](#)[▶](#)[Back](#)[Close](#)[Full Screen / Esc](#)[Printer-friendly Version](#)[Interactive Discussion](#)

Ice nucleation of
bacterial cells

O. Möhler et al.

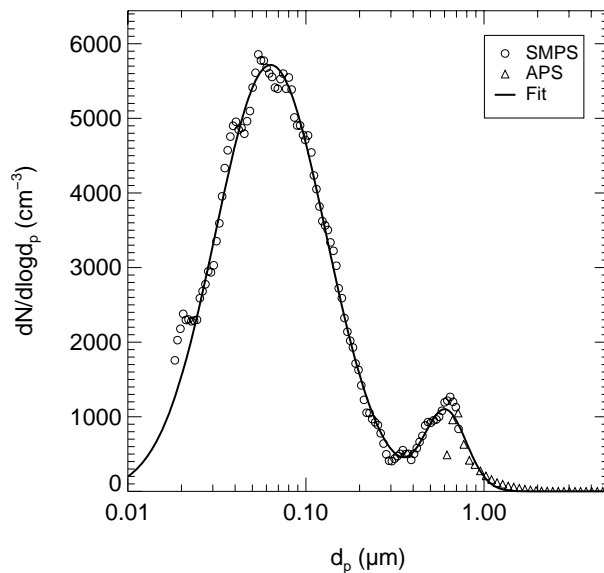


Fig. 3. Same as Fig. 2 for *P. syringae 31R1* of experiment Bio03_09. In this example the mode of bacterial cell particles has a median diameter of 0.6 μm

[Title Page](#)[Abstract](#)[Introduction](#)[Conclusions](#)[References](#)[Tables](#)[Figures](#)[I ◀](#)[▶ I](#)[◀](#)[▶](#)[Back](#)[Close](#)[Full Screen / Esc](#)[Printer-friendly Version](#)[Interactive Discussion](#)

Ice nucleation of bacterial cells

O. Möhler et al.

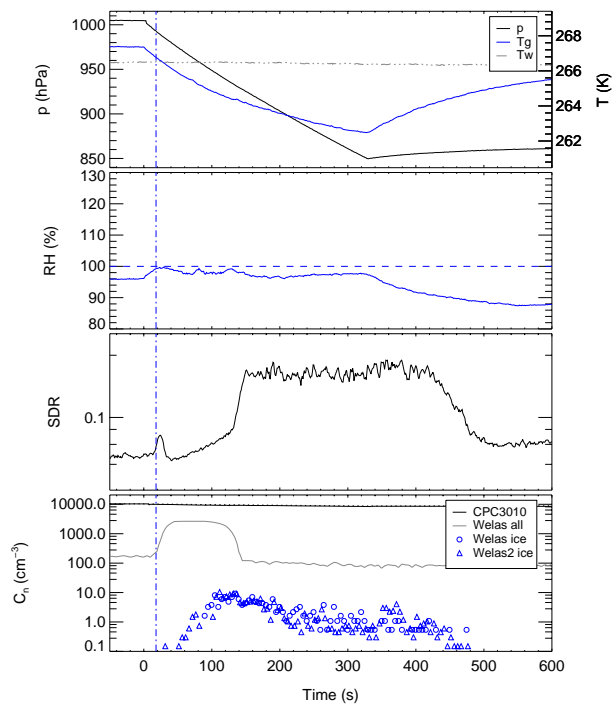


Fig. 4. Time series of data from expansion experiment Bio03_07 with Snomax™ aerosol.

Title Page

Abstract

Introduction

Conclusions

References

Tables

Figures

◀

▶

◀

▶

Back

Close

Full Screen / Esc

Printer-friendly Version

Interactive Discussion



Ice nucleation of bacterial cells

O. Möhler et al.

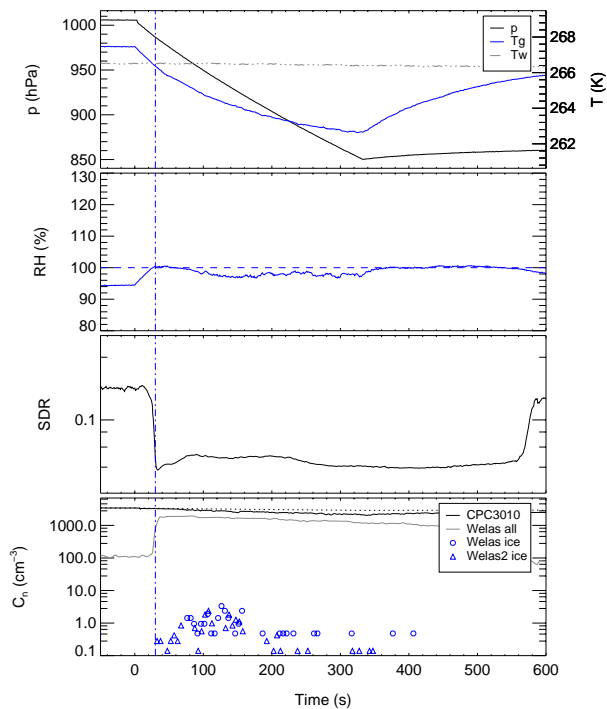


Fig. 5. Time series of data from expansion experiment Bio03_09 with strain 31R1 aerosol.

Title Page

Abstract

Introduction

Conclusions

References

Tables

Figures

◀

▶

◀

▶

Back

Close

Full Screen / Esc

Printer-friendly Version

Interactive Discussion

